Evolution of Echocardiography-Derived Hemodynamic Force Parameters After Cardiac Resynchronization Therapy

Dorien Laenens, MD[a], Pieter van der Bijl, MD, PhD[a], Xavier Galloo, MD[a,b], Alessandro C. Rossi, PhD[c], Giovanni Tonti, MD, PhD[d], Johan H. Reiber, PhD[c,e], Gianni Pedrizzetti, PhD[f,g], Nina Ajmone Marsan, MD, PhD[a], and Jeroen J. Bax, MD, PhD[a,h,*]

Echocardiography-derived hemodynamic forces (HDF) allow calculation of intraventricular pressure gradients from routine transthoracic echocardiographic images. The evolution of HDF after cardiac resynchronization therapy (CRT) has not been investigated in large cohorts. The aim was to assess HDF in patients with heart failure implanted with CRT versus healthy controls. HDF were assessed before and 6 months after CRT. The following HDF parameters were calculated: (1) apical-basal strength, (2) lateral-septal strength, (3) the ratio of lateral-septal to apical-basal strength ratio, and (4) the force vector angle (1 and 2 representing the magnitude of HDF, 3 and 4 representing the orientation of HDF). In the propulsive phase of systole, the apical-basal impulse and the systolic force vector angle were measured. A total of 197 patients were included (age 64 ± 11 years, 62% male), with left ventricular ejection fraction ≤35%, QRS duration ≥130 ms and left bundle branch block. The magnitude of HDF was significantly lower and the orientation was significantly worse in patients with heart failure versus healthy controls. Immediately after CRT implantation, the apical-basal impulse and systolic force vector angle were significantly increased. Six months after CRT, improvement of apical-basal strength, lateral-septal to apical-basal strength ratio and the force vector angle occurred. When CRT was deactivated at 6 months, the increase in the magnitude of apical-basal HDF remained unchanged while the systolic force vector angle worsened significantly. In conclusion, HDF in CRT recipients reflect the acute effect of CRT and the effect of left ventricular reverse remodeling on intraventricular pressure gradients. Whether HDF analysis provides incremental value over established echocardiographic parameters, remains to be determined. **(Am J Cardiol 2023;209:138−145)**

Keywords: cardiac resynchronization, fluid dynamics, heart failure, hemodynamic forces

Echocardiography-derived hemodynamic forces (HDFs) are a new technique to evaluate intracardiac fluid dynamics noninvasively.[1] Blood flow is driven by HDF and changes in HDF may reveal pathologic alterations even before myocardial deformation occurs. A recently developed mathematical formula, based on endocardial tissue movement tracking and the areas of the mitral and aortic valve orifices, allows calculation of HDF in the left ventricle (LV) without flow measurements.[2] Dedicated software (QStrain Echo 4.1.4.4., Medis Suite Ultrasound; Medis Medical Imaging, Leiden, The Netherlands) incorporates this formula and enables calculation of HDF from routine transthoracic echocardiographic images using speckle tracking technology. The technique has been validated against 4-dimensional flow cardiac magnetic resonance imaging.[3] HDF parameters are displayed as time-dependent curves and polar histograms (Figures 1 and 2), which provide insight into the magnitude and the orientation of HDF in the LV. HDF calculation has been applied in different pathologies and provides better understanding of the hemodynamic changes in these conditions.[4] However, this technique has not been evaluated in large and homogeneous patient cohorts. Patients eligible for cardiac resynchronization therapy (CRT) experience intra- and interventricular conduction delays which induce mechanical dyssynchrony and severely impair the generation of adequate HDF. The evolution of HDF over time in CRT recipients has not been investigated. CRT reverses the conduction delay by means of biventricular pacing, and consequently HDF change significantly. These alterations can be investigated by

[a]Departments of Cardiology, Leiden University Medical Centre, Leiden, The Netherlands; [b]Department of Cardiology, University Hospital Brussels, Vrije Universiteit Brussel, Brussels, Belgium; [c]Ultrasound Department, Medis Medical Imaging, Leiden, The Netherlands; [d]Cardiology Division, G. D'Annunzio University, Chieti, Italy; [e]Department of Radiology, Leiden University Medical Centre, Leiden, The Netherlands; [f]Department of Engineering and Architecture, University of Trieste, Trieste, Italy; [g]Department of Biomedical Engineering, University of California, Irvine, California; and [h]Department of Cardiology, Turku Heart Center, University of Turku and Turku University Hospital, Turku, Finland. Manuscript received July 18, 2023; revised manuscript received and accepted September 27, 2023.

Funding: none.

See page 144 for Declaration of Competing Interest.

*Corresponding author: Tel: +31 71 526 2020.

E-mail address: j.j.bax@lumc.nl (J.J. Bax).

https://doi.org/10.1016/j.amjcard.2023.09.098

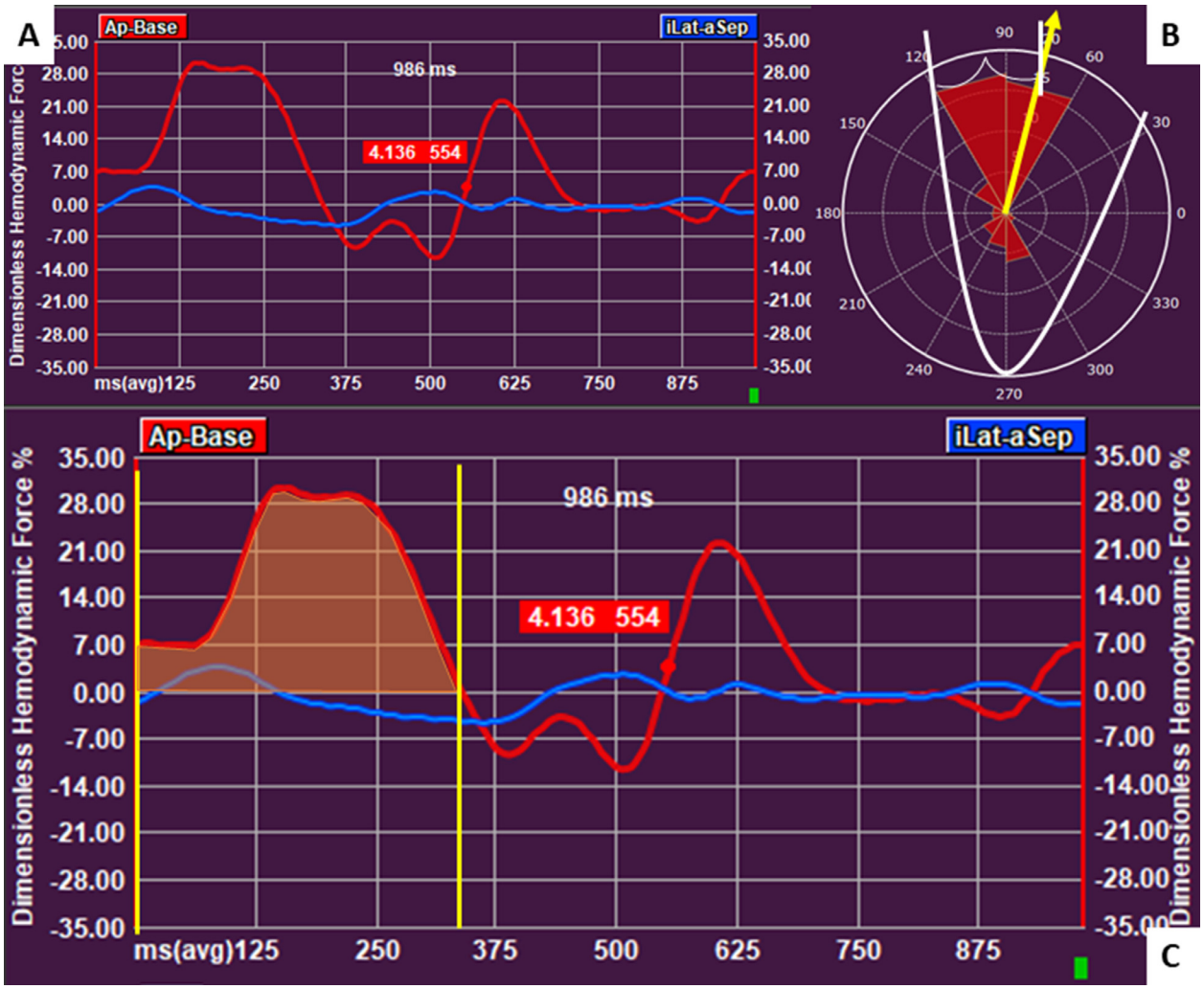

Figure 1. HDF analysis in a healthy control (*A*) The red curve represents the apical-basal HDFs. The apical-basal strength is 14% in this example. The blue curve represents the lateral-septal HDF. The lateral-septal strength is 2% in this example. (*B*) The polar histogram represents the distribution of magnitude and orientation of HDF during the heart cycle. The yellow arrow represents the force vector angle and is 77˚ in this example. (*C*) The systolic thrust = positive part of systole, indicated by the yellow lines. The orange part represents the apical-basal impulse of the systolic thrust (19% in this example).

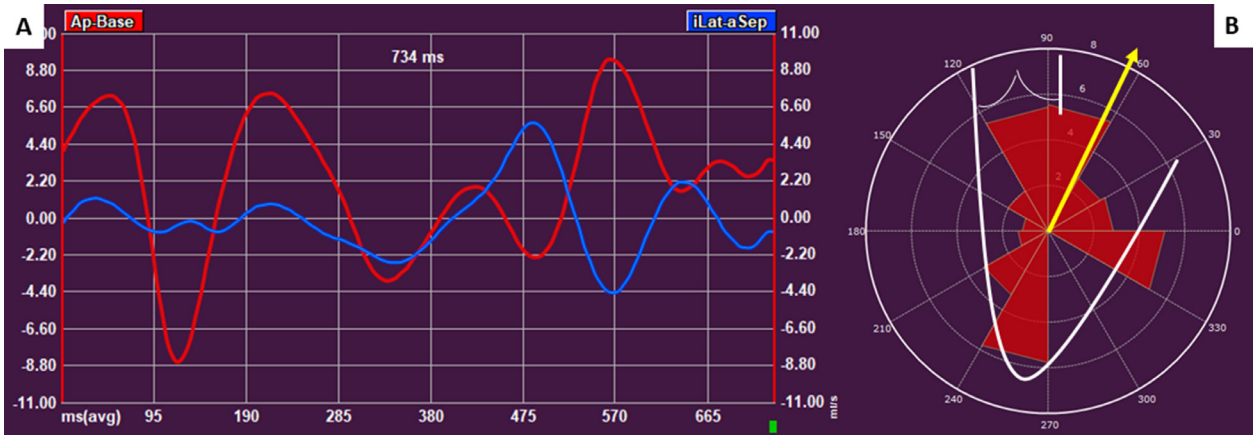

Figure 2. Hemodynamic force analysis in a patient with nonischemic cardiomyopathy and left bundle branch block before CRT implantation(*A*) The red curve represents the apical-basal HDFs. The apical-basal strength is 5% in this patient. The blue curve represents the lateral-septal HDF. The lateral-septal strength is 2% in this patient. (*B*) The polar histogram represents the distribution of magnitude and orientation of HDF during the heart cycle. The yellow arrow represents the force vector angle and is 63˚ in this example.

echocardiography-derived HDF assessment before and after CRT implantation.[5] Furthermore, the change of HDF 6 months after CRT (with potential LV reverse remodeling), has not been documented thus far. Therefore, the aim of the present study was twofold, (1) to assess echocardiography-derived HDF in a homogeneous patient cohort who underwent CRT implantation and to compare these HDF parameters with the values in healthy controls; (2) to explore the evolution of HDF immediately and 6 months after CRT implantation and after temporary deactivation of the CRT device at 6 months.

Methods

Patients were selected from a CRT database. In order to select a homogeneous patient population, patients with heart failure secondary to nonischemic cardiomyopathy (to avoid scar that might influence HDF), with LV ejection fraction (LVEF) ≤35%, QRS duration ≥130 ms and left bundle branch block (to avoid the influence of different activation patterns of the LV on HDF) were included in this analysis (Supplementary Figure 1). All patients had a class I level A or class IIa level B indication for CRT implantation according to current heart failure guidelines.[6] They were implanted with a CRT device between September 2000 and September 2014 at the Leiden University Medical Center, The Netherlands. The mathematical model used to calculate HDF, incorporates the movement of the endocardial border and the area of the mitral and the aortic valve. The area of the aortic valve is estimated using the LV outflow tract (LVOT) diameter and has assumptions. Therefore, patients with significant aortic stenosis (aortic valve area ≤1.5 cm^2) and insufficient imaging quality to track the endocardial border were excluded. In addition, patients with clinically significant mitral stenosis were excluded. The heart failure patients were matched with healthy controls according to age, gender and body mass index. From these matched controls, 30 healthy subjects were randomly selected as a control group for HDF assessment. In CRT recipients, demographic, clinical, electrocardiographic, and echocardiographic data were prospectively collected before CRT implantation in the departmental cardiology information system (EPD-vision; Leiden University Medical Center) and retrospectively analyzed. Quality of life was assessed by the Minnesota Living with Heart Failure Questionnaire. A 6-minute walk test was performed to evaluate exercise capacity. The study complies with the Declaration of Helsinki and was approved by the Institutional Review Board. Because of the retrospective design of this study, the need for written informed consent was waived by the local ethics committee.

Transthoracic echocardiography was performed in all patients before CRT implantation, immediately after CRT implantation, and 6 months after CRT implantation with the CRT device turned on and off with commercially available ultrasound equipment (Vivid 7 and E9; GE-Vingmed, Horten Norway). Echocardiographic data were digitally stored for offline analysis using EchoPAC version 203 (GE Medical Systems, Horten, Norway). LV volumes were measured from the apical 4- and 2-chamber views according to current recommendations and indexed to body surface area.[7] Simpson's biplane method was used to calculate LVEF.[7] LV global longitudinal strain (LV GLS) was measured using speckle tracking strain analysis. The region of interest was automatically created and manually adjusted. LV GLS was then calculated by averaging the peak longitudinal strain values of the 17 segments, excluding segments that could not be traced correctly. The values of LV GLS are reported as absolute values. The severity of mitral regurgitation was graded using a multiparametric approach.[8,9] First, the color flow of the regurgitant jet was evaluated. When considered more than mild mitral regurgitation, the vena contracta width, E-wave velocity, and the pulsed Doppler of the pulmonary veins were assessed. Moderate to severe mitral regurgitation was considered significant.

HDF analysis was performed on the following 4 different time points: (1) at baseline pre-CRT, (2) at baseline post-CRT, (3) at 6 months with CRT-ON and (4) at 6 months with CRT-OFF. The 4-, 3- and 2-chamber apical views were analyzed with novel proprietary software (QStrain Echo 4.1.4.4., Medis Suite Ultrasound; Medis Medical Imaging, Leiden, The Netherlands), and the endocardial border was traced at LV end-systole and LV end-diastole. The mitral valve opening was estimated by measuring the opening of the valve at the tip of the leaflets on the apical 4-chamber view. The aortic valve opening was estimated using the LVOT diameter, measured on the parasternal long-axis view. The software automatically calculated the HDF parameters using a validated formula based on the velocity at the LV endocardium and the velocity across the mitral and aortic valves.[3] The following HDF parameters were calculated for the complete heart cycle (Figure 1): (1) apical-basal strength, represented as the red curve; (2) lateral-septal strength, represented as the blue curve; (3) the ratio of lateral-septal strength to apical-basal strength (LS-AB ratio) and (4) the force vector angle, represented as the yellow arrow in the polar histogram. The strength parameters reflect the magnitude of the force in the longitudinal (apical-basal strength) and transverse (lateral-septal strength) direction. The LS-AB ratio and the angle reflect the orientation of force, with an angle of 90° indicating that the force is perfectly along the base-apex direction. The amplitude of the apical-basal strength and lateral-septal strength is reported as a root mean square value, including both positive and negative values, corrected for LV volume and adjusted for gravity acceleration and fluid density. These parameters are presented as percentages, allowing comparison among subjects. Next, the systolic thrust was defined based on previously described physiological patterns in the apical-basal direction (red curve) (Figure 1).[1,4] The systolic thrust is the first positive part of the red curve, representing the propulsive phase of systole in which the longitudinal force is directed toward the LVOT. In this phase, the apical-basal impulse and systolic force vector angle are measured. The apical-basal impulse is the area under the curve and reflects the magnitude of the apical-basal force in this phase of the cardiac cycle. Correcting for LV volume and adjusting for gravity acceleration and fluid density also allows representation as a dimensionless number.

CRT implantation was performed with a standard approach, that is, by insertion of the right atrial and right ventricular leads by way of the subclavian or cephalic veins. Before insertion of the LV lead, a venography of the coronary sinus was performed. The LV pacing lead was then introduced through an 8Fr guiding catheter and positioned in a posterior or posterolateral branch of the coronary sinus, if possible. A posterior or lateral lead position was accomplished in 77% of the patients with available information about LV lead placement. A total of 97% of the implanted devices had defibrillator functionality. CRT recipients were followed up at regular intervals at the heart failure outpatient clinic, where the device was interrogated. Atrioventricular and interventricular delays were empirically set at 120 to 140 and 0 ms, respectively. CRT optimization occurred at the discretion of the treating physician.

Continuous variables are presented as mean ± SD when normally distributed and as median with interquartile range when not normally distributed. Categorical variables are presented as numbers with percentages. Independent Student *t* test and Mann-Whitney U test were used to compare baseline HDF parameters between heart failure patients and healthy controls. Paired *t* test and Wilcoxon signed rank test were used to compare measurements within heart failure patients. Repeated measurements analysis of variance was used to compare measurements at 4 different time points. In total, 15 random echocardiographic examinations were selected for the evaluation of intra- and interobserver variability of HDF parameters, using intraclass correlation coefficients. Excellent agreement was defined by an intraclass correlation coefficient >0.90, whereas good agreement was defined by a value between 0.75 and 0.90. All tests were two-sided, and p <0.05 were considered statistically significant. All analyses were performed using SPSS Statistics for Windows, version 25.0 (IBM, Armonk, New York).

Results

In total, 197 patients were included in the analysis (Supplementary Figure 1). Baseline characteristics are presented in Table 1. The mean age was 64 ± 11 years, and 122 patients (62%) were male. As compared with healthy controls, the magnitude of the forces in both directions are significantly lower in heart failure patients (Figure 2). The LS-AB ratio is significantly higher and the angle significantly lower in CRT recipients as compared with healthy controls, indicating an abnormal orientation or misalignment of HDF in patients with heart failure before CRT implantation. Also, the apical-basal impulse in the systolic thrust is significantly lower in heart failure patients as compared with healthy controls, reflecting lower apical-basal forces in the propulsive phase of systole. Finally, the systolic force vector angle is lower, indicating an abnormal orientation of HDF in the propulsive phase of systole in patients with heart failure as compared with healthy controls.

The evolution of HDF shortly after CRT implantation is presented in Figure 3, Table 2. During the systolic thrust, there is a significant increase in apical-basal impulse and systolic force vector angle after the onset of CRT. This indicates that the magnitude of the apical-basal forces in the first ejection phase of systole is immediately increased and the direction of HDF in this phase is instantly better aligned with the base-apex direction after onset of CRT. Over the complete cardiac cycle, no significant differences are observed in the HDF parameters, suggesting that the initial changes in HDF after CRT implantation are limited to the systolic phase of the heart cycle.

Table 3 demonstrates the evolution of clinical, echocardiographic, and HDF parameters 6 months after CRT implantation. Patients with heart failure show a significant clinical response to CRT, reflected by the improvement in New York Heart Association class, quality of life and 6-

Table 1
Baseline clinical and echocardiographic characteristics

Variable	CRT recipients Baseline pre CRT (N = 197) N = 196	Healthy controls (N = 30)	p value
Clinical characteristics			
Age, years	63.8 ± 10.5	65.7 ± 8.3	0.347
Male, N (%)	122 (62.2%)	15 (50.0%)	0.213
Body mass index, kg/m^2	26.1 ± 4.6	25.6 ± 4.0	0.545
Arterial hypertension, N (%)	78 (39.8%)		
Diabetes mellitus, N (%)	28 (14.3%)		
Dyslipidemia, N (%)	48 (24.6%)		
Current smoker, N (%)	35 (18.1 %)		
NYHA III or IV, N (%)	128 (65.6%)		
Quality of Life	29.0 (16.0, 44.5)		
6-minute walk test, m	368.0 ± 117.6		
Laboratory results			
Hemoglobin, mmol/l	8.4 ± 0.9		
eGFR MDRD, mg/dl	70.6 ± 22.9		
ECG variables			
Sinus rhythm, N (%)	180 (91.8%)		
Atrial fibrillation, N (%)	15 (7.7%)		
Pacemaker, N (%)	1 (0.5%)		
QRS duration, ms	166.3 ± 20.2		
Medication			
Beta blocker, N (%)	160 (81.6%)		
ACE-I/ARB, N (%)	178 (90.8%)		
Loop diuretic, N (%)	153 (78.1%)		
MRA, N (%)	92 (46.9%)		
Echocardiographic characteristics			
LV end-diastolic volume, ml	214.8 ± 80.4	61.7 ± 18.3	**<0.001**
LV end-systolic volume, ml	162.1 ± 66.9	24.5 ± 9.3	**<0.001**
LV ejection fraction, %	25.3 ± 6.3	60.8 ± 7.0	**<0.001**
LV global longitudinal strain, %	7.2 ± 3.0	18.7 ± 2.2	**<0.001**
Moderate or severe MR, N (%)	78 (42.2 %)	0 (0%)	**<0.001**
Hemodynamic force parameters			
Complete heart cycle			
Apical-basal strength, %	4.8 (3.5, 6.4)	9.5 (7.3, 13.8)	**<0.001**
Lateral-septal strength, %	1.6 (1.1, 2.0)	2.1 (1.6, 3.6)	**<0.001**
LS-AB ratio	32.1 (25.6, 42.2)	24.6 (20.6, 27.7)	**<0.001**
Angle, °	66.2 ± 6.1	71.8 ± 3.4	**<0.001**
Systolic thrust			
Apical-basal impulse, %	4.8 (3.3, 6.5)	10.1 (7.9, 16.5)	**<0.001**
Angle, °	74.0 (70.0, 78.0)	77.0 (74.8, 80.3)	**<0.001**

ACE-I = angiotensin converting enzyme inhibitor; ARB = angiotensin receptor blocker; eGFR MDRD = estimated glomerular filtration rate by Modification of Diet in Renal Disease; LS-AB ratio = lateral-septal strength to apical-basal strength ratio; LV = left ventricular; MR = mitral regurgitation; MRA = mineralocorticoid receptor antagonist; NYHA = New York Heart Association.

Bold values represent significant p values (i.e. <0.05).

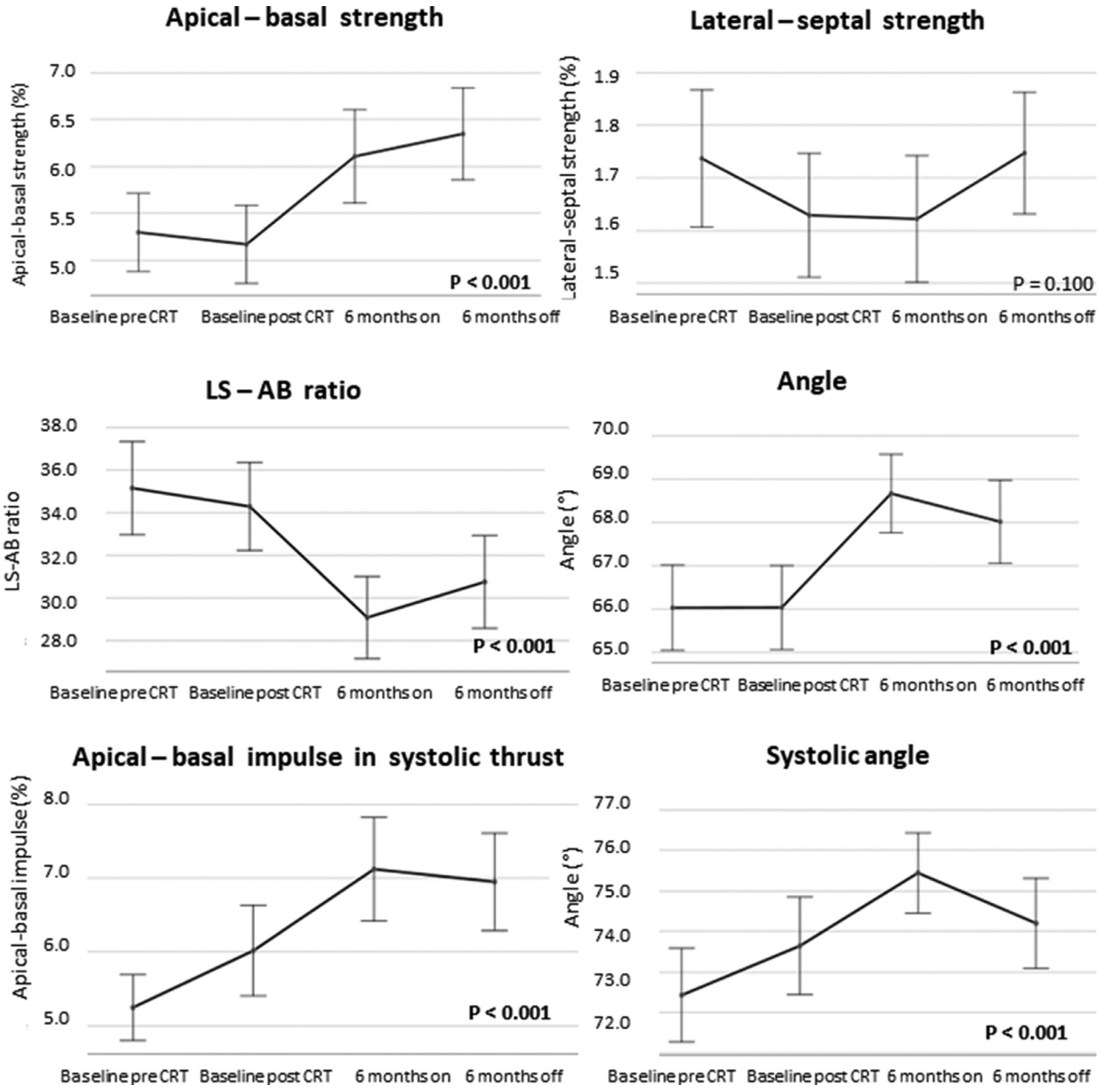

Figure 3. Evolution of HDF parameters at baseline and after 6 months. LS-AB = lateral−septal strength to apical-basal strength ratio

minute walking distance. Substantial LV reverse remodeling is noted, reflected by a significant reduction of LV volumes, significant increase in LVEF and LV GLS with a reduction in significant mitral regurgitation. The evolution of the HDF parameters in the complete heart cycle shows a significant increase in apical-basal strength and a significantly improved alignment of the HDF toward the apex-base direction, reflected in a lower LS-AB ratio and increased force vector angle (Figure 3). The magnitude of the apical-basal impulse and the systolic force vector angle further increases after 6 months (Figure 3).

Changes in HDF parameters after deactivating the CRT device at 6 months are presented in Figure 3, Table 4. The magnitude of the lateral-septal strength increases significantly, indicating a return of lateral-septal forces with recurrent mechanical dyssynchrony. There is a trend toward reduction of the LS-AB ratio and increase of the force vector angle, indicating recurrent misalignment of HDF. The magnitude of the apical-basal strength over the complete cardiac cycle and the magnitude of the apical-basal impulse during the systolic thrust remain unchanged, indicating that LV reverse remodeling is predominantly responsible for the gain in magnitude of apical-basal force after CRT implantation. The force vector angle during the systolic thrust is significantly increased after deactivating the CRT device, also indicating a recurrent misalignment of HDF in this phase of the cardiac cycle.

The intra- and interobserver reproducibility of HDF parameters is summarized in Supplementary Table 1. The agreement is excellent for the HDF parameters measured

Table 2
Evolution of hemodynamic forces immediately after cardiac resynchronization therapy implantation in patients with heart failure

HDF parameter	Baseline pre CRT	Baseline post CRT	p value
Complete heart cycle			
Apical-basal strength, %	4.8 (3.5, 6.4)	4.5 (3.5, 6.3)	0.748
Lateral-septal strength, %	1.6 (1.1, 2.0)	1.5 (1.1, 1.9)	0.092
LS-AB ratio	32.1 (25.6, 42.2)	32.4 (24.6, 40.9)	0.340
Angle, ˚	66.0 ± 6.1	66.3 ± 6.0	0.771
Systolic thrust			
Apical-basal impulse, %	4.8 (3.3, 6.5)	5.3 (3.2, 8.0)	**0.002**
Angle, ˚	74.0 (70.0, 77.0)	75.0 (70.0, 79.0)	**0.036**

LS-AB ratio = lateral-septal strength to apical-basal strength ratio.
Bold values represent significant p values (i.e. <0.05).

Table 3
Evolution of parameters 6 months after cardiac resynchronization therapy implantation in patients with heart failure

Variable	Baseline pre CRT	6 months CRT ON	p value
NYHA class	2.6 ± 0.7	1.9 ± 0.7	**<0.001**
Quality of Life	31.7 ± 19.6	18.3 ± 17.8	**<0.001**
6-minute walk test, m	367.5 ± 117.4	436.0 ± 109.0	**<0.001**
LV end-diastolic volume, ml	214.8 ± 80.4	181.9 ± 84.8	**<0.001**
LV end-systolic volume, ml	162.1 ± 66.9	122.8 ± 70.9	**<0.001**
LV ejection fraction, %	25.3 ± 6.3	34.7 ± 9.8	**<0.001**
LV global longitudinal strain, %	7.3 ± 3.0	9.5 ± 4.0	**<0.001**
Moderate or severe MR, No %	78 (42.2 %)	42 (21.3%)	**<0.001**
Hemodynamic force parameters			
Complete heart cycle			
Apical-basal strength, %	4.8 (3.5, 6.3)	5.6 (4.0, 7.3)	**<0.001**
Lateral-septal strength, %	1.6 (1.1, 2.0)	1.4 (1.1, 2.0)	0.078
LS-AB ratio	32.1 (25.6, 42.2)	26.9 (21.3, 36.4)	**<0.001**
Angle, ˚	66.1 ± 6.1	68.5 ± 5.8	**<0.001**
Systolic thrust			
Apical-basal impulse, %	4.8 (3.3, 6.4)	6.4 (4.0, 9.3)	**<0.001**
Angle, ˚	74.0 (69.0, 78.0)	76.0 (72.0, 79.0)	**<0.001**

Bold values represent significant p values (i.e. <0.05).
NYHA = New York Heart Association; LS-AB ratio = lateral-septal strength to apical-basal strength ratio; LV = left ventricular; MR = mitral regurgitation.

over the complete cardiac cycle, the apical-basal impulse during the systolic thrust (interobserver), and the systolic force vector angle (intraobserver). The agreement is good for the apical-basal impulse during the systolic thrust (intraobserver) and the force vector angle during the systolic thrust (interobserver).

Discussion

The present study includes a large and homogenous patient cohort with heart failure, reduced LVEF secondary to nonischemic cardiomyopathy, and left bundle branch block who underwent CRT device implantation. HDF

Table 4
Evolution of HDF parameters at 6 months after temporary deactivating the CRT device in patients with heart failure

HDF parameter	6 months CRT ON	6 months CRT OFF	p value
Complete heart cycle			
Apical-basal strength, %	5.7 (4.1, 7.3)	5.7 (4.0, 7.7)	0.405
Lateral-septal strength, %	1.4 (1.1, 2.0)	1.6 (1.2, 2.1)	**0.007**
LS-AB ratio	26.6 (21.2, 34.5)	27.9 (20.9, 36.6)	0.053
Angle, ˚	68.7 ± 5.6	68.0 ± 5.9	0.085
Systolic thrust			
Apical-basal impulse, %	6.4 (4.0, 9.2)	6.6 (3.7, 9.4)	0.384
Angle, ˚	77.0 (73.0, 80.0)	75.0 (71.0, 79.0)	**0.016**

Bold values represent significant p values (i.e. <0.05).
LS-AB ratio = lateral-septal strength to apical-basal strength ratio.

analysis at 4 different time points revealed the following findings: (1) the magnitude and orientation of HDF is significantly worse in heart failure patients versus healthy controls; (2) immediately after CRT implantation, improvement of magnitude and orientation of HDF is observed during the systolic thrust; (3) 6 months after CRT, improvement in magnitude and orientation of HDF is visible over the complete cardiac cycle and during the systolic thrust and (4) when the CRT device is temporarily deactivated after 6 months, the orientation of HDF during the systolic thrust worsens while the increase in the magnitude of apical-basal HDF remains maintained.

Intraventricular pressure gradients are the driving force of blood flow, and HDF reflect these pressure gradients. With the use of a new mathematical model, novel dedicated software is able to calculate HDF from routinely acquired echocardiographic images, permitting the use of HDF in clinical practice. The software displays HDF as time-dependent curves and polar histograms that facilitate the clinical interpretation. The curve representing the apical-basal HDF (red curve in Figures 1 and 2), provides information about the magnitude, evolution, and timing of HDF in the longitudinal direction, which is the predominant force in healthy subjects.[1] The blue curve represents the lateral-septal or transverse HDF and becomes more prominent in the presence of ventricular dyssynchrony.[1] The orientation of HDF can be presented using the LS-AB ratio or the force vector angle, visualized as the yellow arrow on the polar histogram (Figures 1 and 2). HDF analysis reveals the direct impact of mechanical dyssynchrony on intraventricular pressure gradients. In the present study, reduced myocardial contractility in heart failure patients is reflected by the reduced magnitude of HDF. Mechanical dyssynchrony, induced by intraventricular and interventricular conduction delays, is reflected in the misalignment of HDF or deviated orientation of HDF (away from the base-apex direction).

CRT reduces conduction delay and LV mechanical dyssynchrony. The effect of CRT on HDF was previously evaluated by Dal Ferro et al[5] in 38 heart failure patients using the same mathematical model as applied in the present study. The authors calculated HDF parameters from transthoracic echocardiographic images, performed within 2 months before and 2 months after CRT implantation. The authors demonstrated a significant improvement in the LS-AB ratio over the complete cardiac cycle after CRT, indicating that CRT causes a beneficial change in the orientation of HDF.[5] Pedrizzetti et al[10] evaluated the effect of CRT on HDF with echocardiographic particle velocimetry imaging. The authors evaluated 30 heart failure patients after 6 months of CRT implantation with the CRT device activated and temporarily turned off. The authors reported a change in the direction of flow momentum after the temporary deactivation of CRT, reflecting a primary effect of CRT on the orientation of HDF.

In the present study, the effect of CRT was comprehensively evaluated using 4 different time points. First, HDF analysis was performed before and immediately after CRT implantation to evaluate the acute effect of CRT on HDF (without any significant impact of LV reverse remodeling). The acute effect of CRT on HDF was clearly demonstrated during the systolic thrust. In this ejection phase during systole, the magnitude of apical-basal HDF and the orientation of HDF improved significantly, suggesting that both the magnitude and orientation of HDF are improved by CRT. This observation agrees with invasive measurements of LV pressure increase immediately after the onset of biventricular pacing.[11,12] Second, 6 months after CRT, HDF analysis revealed not only an improvement in the systolic thrust, but also in the hemodynamics of the complete cardiac cycle. This observation indicates that the beneficial changes in HDF caused by CRT over time cannot solely be attributed to systole, but also to a mechanical advantage in diastole. Third, the CRT device was temporarily deactivated during the echocardiographic examination, and the HDF analysis was repeated. No changes in the magnitude of apical-basal HDF were observed, but a significant deviation of the orientation of HDF during the systolic thrust and a significant increase of lateral-septal HDF over the complete heart cycle were noted. This finding indicates that the gain in the magnitude of apical-basal HDF after 6 months is mainly related to LV reverse remodeling, whereas the recurrent electromechanical dyssynchrony mainly affects the orientation of HDF.

Echocardiography-derived HDF is easily applicable to clinical practice. It is based on speckle tracking technology, which is embedded in the clinical routine of measuring LV GLS. HDF analysis reveals acute changes in fluid dynamics after CRT activation and therefore has the ability to guide CRT implantation and (if needed) CRT optimization. Whether HDF analysis provides incremental value over established echocardiographic parameters, remains to be determined.

The current analysis was a retrospective, single-center study. HDF analysis was limited to the complete heart cycle and the first part of systole. Detailed analysis of HDF in diastole was not included and should be investigated in further studies.

Echocardiography-derived HDF provides insight into the magnitude and orientation of intraventricular pressure gradients in patients with heart failure. HDF analysis reveals the acute effect of CRT on the magnitude and orientation of HDF during the systolic thrust, the effect on magnitude and orientation over the complete cardiac cycle after 6 months and helps to differentiate the acute effect of CRT versus the late effect of LV reverse remodeling (at 6 months).

Data Availability

The data underlying this article will be shared on reasonable request by the corresponding author.

Declaration of Competing Interest

The Department of Cardiology of Leiden University Medical Center received research grants from Abbott Vascular, Bayer, Biotronik, Bioventrix, Boston Scientific, Edwards Lifesciences, GE Healthcare (Little Chalfont, United Kingdom), Medis Medical Imaging, Medtronic, and Novartis. Jeroen J. Bax received speaker fees from Abbott Vascular, Edwards Lifesciences, and Omron. Nina Ajmone Marsan received speaker fees from Abbott Vascular and GE Healthcare. The remaining authors have no competing interests to declare.

Supplementary materials

Supplementary material associated with this article can be found in the online version at https://doi.org/10.1016/j.amjcard.2023.09.098.

1. Vallelonga F, Airale L, Tonti G, Argulian E, Milan A, Narula J, Pedrizzetti G. Introduction to hemodynamic forces analysis: moving into the new frontier of cardiac deformation analysis. *J Am Heart Assoc* 2021;10:e023417.
2. Pedrizzetti G. On the computation of hemodynamic forces in the heart chambers. *J Biomech* 2019;95:109323.
3. Pedrizzetti G, Arvidsson PM, Töger J, Borgquist R, Domenichini F, Arheden H, Heiberg E. On estimating intraventricular hemodynamic forces from endocardial dynamics: a comparative study with 4D flow MRI. *J Biomech* 2017;60:203–210.
4. Laenens D, van der Bijl P, Stassen J, Rossi AC, Pedrizzetti G, Reiber JHC, Marsan NA, Bax JJ. Introduction to hemodynamic forces by echocardiography. *Int J Cardiol* 2023;370:442–444.
5. Dal Ferro M, De Paris V, Collia D, Stolfo D, Caiffa T, Barbati G, Korcova R, Pinamonti B, Zovatto L, Zecchin M, Sinagra G, Pedrizzetti G. Left ventricular response to cardiac resynchronization therapy: insights from hemodynamic forces computed by speckle tracking. *Front Cardiovasc Med* 2019;6:59.
6. McDonagh TA, Metra M, Adamo M, Gardner RS, Baumbach A, Böhm M, Burri H, Butler J, Čelutkienė J, Chioncel O, Clelenad JGF, Coats AJS, Crespo-Lerio MG, Farmakis D, Gilard M, Heymans S, Hoes AW, Jaarsma T, Jankowska EA, Lainscak M, Lam CSP, Lyon AR, McMurray JJV, Mebazaa A, Mindham R, Muneretto C, Francesco Piepoli MF, Price S, Rosano GMC, Ruschitzka F, Kathrine Skibelund A, ESC Scientific Document Group. 2021 ESC Guidelines for the diagnosis and treatment of acute and chronic heart failure. *Eur Heart J* 2021;42:3599–3726.
7. Lang RM, Badano LP, Mor-Avi V, Afilalo J, Armstrong A, Ernande L, Flachskampf FA, Foster E, Goldstein SA, Kuznetsova T, Lancellotti P, Muraru D, Picard MH, Rietzschel ER, Rudski L, Spencer KT, Tsang W, Voigt JU. Recommendations for cardiac chamber quantification by echocardiography in adults: an update from the American Society of Echocardiography and the European Association of Cardiovascular Imaging. *J Am Soc Echocardiogr* 2015;28:1–39. .e14.
8. Lancellotti P, Tribouilloy C, Hagendorff A, Popescu BA, Edvardsen T, Pierard LA, Badano L, Zamorano JL. Scientific Document Committee of the European Association of Cardiovascular Imaging. Recommendations for the echocardiographic assessment of native valvular regurgitation: an executive summary from the European Association of Cardiovascular Imaging. *Eur Heart J Cardiovasc Imaging* 2013;14:611–644.
9. Zoghbi WA, Adams D, Bonow RO, Enriquez-Sarano M, Foster E, Grayburn PA, Hahn RT, Han Y, Hung J, Lang RM, Little SH, Shah DJ, Shernan S, Thavendiranathan P, Thomas JD, Weissman NJ. Recommendations for noninvasive evaluation of native valvular regurgitation: a report from the American Society of Echocardiography developed in collaboration with the Society for Cardiovascular Magnetic Resonance. *J Am Soc Echocardiogr* 2017;30:303–371.
10. Pedrizzetti G, Martiniello AR, Bianchi V, D'Onofrio A, Caso P, Tonti G. Changes in electrical activation modify the orientation of left ventricular flow momentum: novel observations using echocardiographic particle image velocimetry. *Eur Heart J Cardiovasc Imaging* 2016;17:203–209.
11. van Gelder BM, Meijer A, Bracke FA. Timing of the left ventricular electrogram and acute hemodynamic changes during implant of cardiac resynchronization therapy devices. *Pacing Clin Electrophysiol* 2009;32(suppl 1):S94–S97.
12. Hamad MA, van Gelder BM, Bracke FA, van Zundert AA, van Straten AH. Acute hemodynamic effects of cardiac resynchronization therapy in patients with poor left ventricular function during cardiac surgery. *J Card Surg* 2009;24:585–590.